Thin Solid Films 595 (2015) 142–147

Contents lists available at ScienceDirect

Thin Solid Films

journal homepage: www.elsevier.com/locate/tsf

# Synthesis and characterization of $Zr_2Al_3C_4$ thin films

Chung-Chuan Lai *, Mark D. Tucker [1], Jun Lu, Jens Jensen, Grzegorz Greczynski, Per Eklund, Johanna Rosen

*Thin Film Physics Division, Department of Physics, Chemistry and Biology (IFM), Linköping University, SE-581 83 Linköping, Sweden*

ARTICLE INFO

*Article history:*
Received 12 June 2015
Received in revised form 7 October 2015
Accepted 30 October 2015
Available online 31 October 2015

*Keywords:*
Thin film
Cathodic arc deposition
Zr2Al3C4
Nanolaminate
Zirconium carbide

ABSTRACT

$Zr_2Al_3C_4$ is an inherently nanolaminated carbide where layers of ZrC alternate with layers of $Al_3C_2$. Characterization of bulk samples has shown it has improved damage tolerance and oxidation resistance compared to its binary counterpart ZrC. Though a potential candidate for coatings applied for use in harsh environments, thin films of $Zr_2Al_3C_4$ have not been reported. We have synthesized epitaxial $Zr_2Al_3C_4$ thin films by pulsed cathodic arc deposition from three elemental cathodes, and have studied the effect of incident atomic flux ratio, deposition temperature, and choice of substrate on material quality. X-ray diffraction analysis showed that $Zr_2Al_3C_4$ of the highest structural quality was obtained for growth on 4 H–SiC(001) substrate at 800 °C. Also, suppression of competing phases could be achieved on $\alpha$-$Al_2O_3$(001) at elevated substrate temperatures. Very similar growth behavior to that of the well-known $M_{n+1}AX_n$ phases – Al supersaturation, binary carbide intergrowth and high sensitivity to choice of substrate – indicates a strong connection between the two families of materials, despite their differences in structure and in chemistry.



## 1. Introduction

The binary transition metal carbides (*MC*, where *M* is a transition metal) have been thoroughly studied since the 1930s, in part motivated by attention from industry [1]. *MC*s are generally harder, more refractory, and more chemically stable than their metallic counterparts, while remaining electrically and thermally conductive, but they are brittle [2]. Today, they are commonly utilized as reinforcement in composites (e.g. WC–Co [3]) and protective coatings (e.g. TiC, NbC, CrC [4]).

In order to improve the performance of binary carbides at elevated temperature, a third component can be introduced, forming ternary transition metal carbides (*MA*C, where *A* is typically a group 13–16 element). Commonly, the *A* element is Al, as in $Ti_2AlC$, $Ti_3AlC_2$ and $Zr_2Al_3C_4$, causing improvement in high temperature oxidation resistance by the formation of a continuous and dense oxygen diffusion barrier of alumina on the surface [5–10].

A class of ternary and quaternary carbides have inherently nanolaminated structures with alternating transition metal carbide layers (*M*C) and *A*-element-containing layers (*A* or *A*C) along one crystal axis [11]. They have several different formulas $M_{n+1}AC_n$, $(MC)_n(A_3C_2)$, and $(MC)_n(A_4C_3)$, where $n$ is 1–3 [12,13], for example $Ti_3AlC_2$, $(ZrC)_2(Al_3C_2)$ or $Zr_2Al_3C_4$, and $(HfC)_3(Al_4C_3)$ or $Hf_3Al_4C_6$ [14–16]. They commonly have superior mechanical properties, such as higher tolerance against damage and increased machinability, to their binary carbide counterparts [14,17,18].These properties originate from their layered structures.

$Zr_2Al_3C_4$ was first reported in bulk form in 1980 by Schuster and Nowotny [19], but detailed studies on properties of this phase were not conducted until the 2000s. The material exhibits high electrical conductivity (1.10 μΩm) along with higher stiffness and toughness than ZrC [20] and an improved high temperature oxidation resistance. Because of these properties, Zhou et al. proposed $Zr_2Al_3C_4$ as a potential candidate for applications such as reinforcing composite for metals [21] and protective conducting coatings in harsh environments [13]. However, thin film synthesis of inherently nanolaminated phases in the Zr–Al–C system, including $Zr_2Al_3C_4$, has not yet been reported.

Here, we report synthesis of $Zr_2Al_3C_4$ thin films by pulsed cathodic arc deposition. Samples deposited with different Al to Zr and C to Zr incident atomic flux ratios, on different substrates ($\alpha$-$Al_2O_3$(001), MgO(111), 4 H–SiC(001), and yttria-stabilized-zirconia (YSZ) (111)), and at different substrate temperatures (700 °C, 750 °C, 800 °C and 900 °C) were investigated. Epitaxial growth of $Zr_2Al_3C_4$ was achieved on 4 H–SiC substrates, and suppression of competing phases could also be achieved on $\alpha$-$Al_2O_3$ at elevated substrate temperatures.

## 2. Experimental details

### 2.1. Thin film synthesis

All depositions were made in a high current pulsed cathodic arc system equipped with three cylindrical cathodes (Ø = 25 mm), slightly tilted to allow plasma flux into a copper solenoid filter for macroparticle removal. This method has previously been used for synthesis of

* Corresponding author.
*E-mail address:* chula@ifm.liu.se (C.-C. Lai).
[1] Current affiliation: Department of Physics and Astronomy, Curtin University, Perth WA 6102, Australia.

http://dx.doi.org/10.1016/j.tsf.2015.10.079
0040-6090/

laminated carbides [22–24], see Ref. [25] for details about the deposition system. Each cathode is surrounded by a cylindrical anode and is triggered using a center-positioned tungsten trigger pin electrically insulated from the cathode. During deposition, the cathodes are fired separately, at a base pressure of around $10^{-7}$ mbar.

The samples were deposited from three elemental cathodes, Zr, Al and C, with purities of 99.9%, 99.99% and 99.99%, respectively (Testbourne Ltd.), using an arc current of 1.5 kA and a pulsed frequency of 11 Hz. The width of one pulse for the Zr, Al and C cathodes were 350, 250 and 500 μs, respectively.

The incoming atomic flux ratio was controlled by triggering the three cathodes in a repeating pulse sequence and varying the number of pulses to each cathode in the sequence. In initial calibrations the deposition rate from each cathode was determined by attaining density and thickness from x-ray reflectivity (XRR) measurements on samples deposited on Si(100) substrates at room temperature. This information was used to determine the atomic flux ratio incident on the substrate (or the 'flux ratio') for a chosen pulse sequence.

The substrates used in this work were α-$Al_2O_3$(001), MgO(111), 4 H–SiC(001), and yttria-stabilized zirconia (111) (YSZ, $Zr_{0.92}Y_{0.08}O_2$). All substrates were cleaned in an ultrasonic bath for 10 min each in acetone then isopropanol, and were blown dry with $N_2$. The substrate was kept for 15 min at the deposition temperature before material synthesis to ensure a uniformr temperature over the sample. One thin film sample, presented in Section 3.1, was deposited on 4 H–SiC(001) with a thickness of about 200 nm for better statistics in composition analysis, see Section 2.2. The other samples presented were about 20 nm thick according to deposition rate calibration prior to the sample deposition.

### 2.2. Thin film characterization

XRR and X-ray diffraction (XRD) patterns were acquired in an X-ray diffractometer (*Empyrean*, *PANalytical B.V.*) using CuKα radiation and a Ge(220) crystal hybrid monochromator on the incident side and a parallel plate collimator (PPC) on the receiving side. An extra equatorial 0.1 mm collimator slit was inserted between the PPC and the detector when acquiring XRR patterns, which later were fitted within X'Pert Reflectivity software (Ver. 1.3, *PANalytical B.V.*) to obtain the density and thickness of the calibration samples. XRD was used for phase indentification and analysis of crystal orientation.

The microstructure of the films was characterized using high-resolution transmission electron microscopy (HR-TEM) on cross-sectional samples in a FEI Tecnai G2 microscope operated with an acceleration voltage of 200 kV.

Time-of-flight elastic recoil detection analysis (TOF-ERDA) was performed on the thicker sample to obtain an average composition from a larger sampling volume and a more reliable quantification of the lighter elements, such as C, O and N.

## 3. Results and discussion

### 3.1. Characterization of $Zr_2Al_3C_4$ thin films

Fig. 1(a) is a $\theta$–$2\theta$ XRD pattern of a $Zr_2Al_3C_4$ thin film deposited on 4 H–SiC(001) at 800 °C with flux ratio (Al/Zr) = 5.75 and (C/Zr) = 1.67. The six diffraction peaks labeled s in Fig. 1 (a) are the basal planes (00 *l*) of the SiC substrate [26]. The eight peaks at around 7.9°, 15.9°, 24.2°, 32.3°, 40.7°, 58.4°, 67.7° and 77.3° share the same least common multiple of interplanar spacing (*d* spacing) ~11.1 Å, and can be assigned to diffraction from the basal planes (00 *l*) of the $Zr_2Al_3C_4$ phase with a *c* parameter of ~22.2 Å [27]. The additional peaks at ~33.0° and ~69.1° are the 111 and 222 peaks of cubic $ZrC_x$ ($0.67 \le x \le 1.0$) [28]. The inset of Fig. 1(a) is an in-plane ($\psi$ ~ 90°) $\theta$–$2\theta$ XRD pattern over the range $2\theta$ = 52–62° showing 110 diffraction of $Zr_2Al_3C_4$ and the substrate. From the position of $Zr_2Al_3C_4$(110) its *a* parameter can be determined to be ~3.34 Å, while the asymmetric shape of the peak indicates an overlap of a $ZrC_x$ 220 peak with lower intensity.

Fig. 1 (b) shows $\varphi$-scans acquired at $2\theta$ = 65.702°, 53.040° and 58.560° and at fixed tilt angle $\psi$ from the surface normal of the sample, with $\psi$ = 68.50°, 55.50° and 63.00°, which correspond to diffraction from $Zr_2Al_3C_4$(103), $Zr_2Al_3C_4$(105) and 4 H–SiC(102) planes, respectively. The six peaks separated by 60° in all three scans share the same $\varphi$ peak positions, indicating the epitaxial relation $Zr_2Al_3C_4$[100] || 4 H–SiC[100] and $Zr_2Al_3C_4$[001] || 4 H–SiC[001].

TOF-ERDA quantification of the sample investigated in Fig. 1 showed average atomic concentrations of (Zr, Al, C, O, N) = (29.3, 26.8, 43.1, 0.6, 0.1) at.%, respectively. Traces of Ti and Hf, which are both common impurities found in Zr cathodes [29], were also observed but at levels below the quantification limit. This data shows that, relative to the composition of $Zr_2Al_3C_4$, the film is deficient in Al, explaining the presence of $ZrC_x$ formed from the excess Zr and C. The nearly 4 times higher (Al/Zr) flux ratio than the stoichiometry of $Zr_2Al_3C_4$ phase, as well as the Al deficiency observed in this film, were likely due to high sublimation rate and low sticking coefficient of Al at 800 °C. The known higher sputter

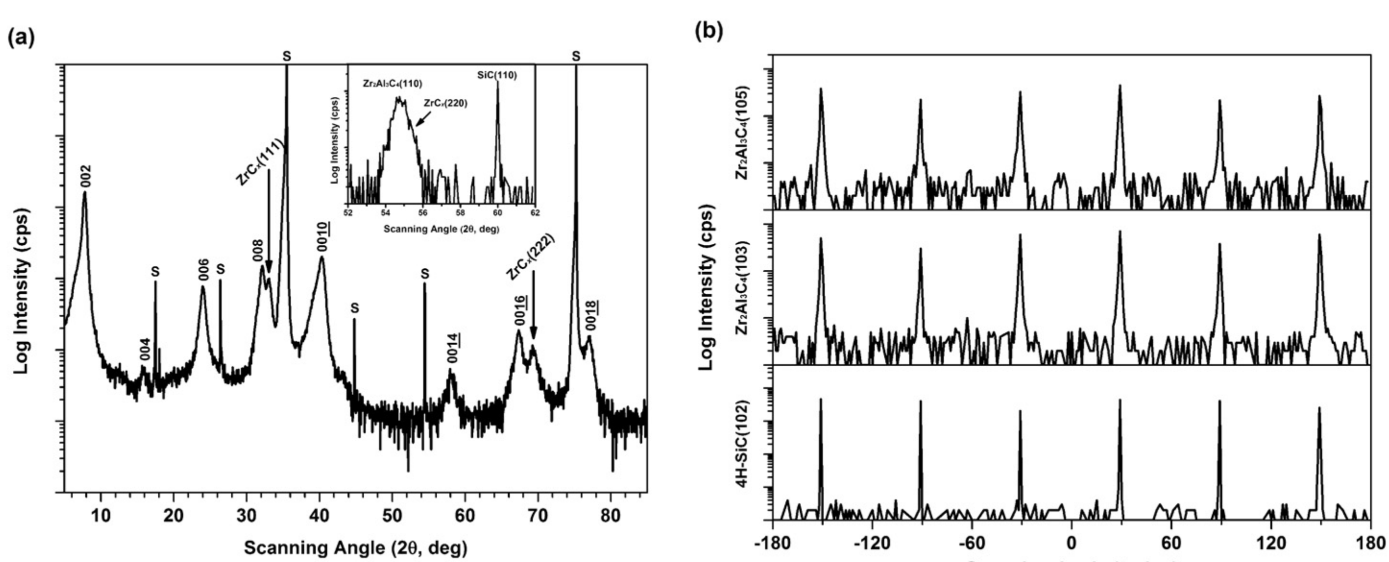


**Fig. 1.** (a) $\theta$–$2\theta$ XRD patterns of a $Zr_2Al_3C_4$ thin film grown on 4 H–SiC(001) at 800 °C. The inset is an in-plane $\theta$–$2\theta$ XRD pattern over the range $2\theta$ = 52–62°. (b) Tilted $\varphi$-scan XRD patterns on the $Zr_2Al_3C_4$(103), $Zr_2Al_3C_4$(105) and 4 H–SiC(102) planes of the sample shown in (a).